www.nature.com/aps

Acta Pharmacologica Sinica

ARTICLE

Costunolide alleviates HKSA-induced acute lung injury via inhibition of macrophage activation

Yun-tian Chen[1], Yao Du[2], Bo Zhao[3], Li-xing Gan[1], Kai-kai Yu[3], Lei Sun[3], Jian Wang[1] and Feng Qian[3]

Staphylococcus aureus (*S. aureus*) infection leads to a severe inflammatory response and causes acute lung injury (ALI), eventually threatening human life. Therefore, it is of importance to find an agent to inhibit inflammation and reduce ALI. Here, we found that costunolide, a sesquiterpene lactone, displays anti-inflammatory effects and ameliorates heat-killed *S. aureus* (HKSA)-induced pneumonia. Costunolide treatment attenuated HKSA-induced murine ALI in which pulmonary neutrophil infiltration was inhibited, lung edema was decreased, and the production of pro-inflammatory cytokines was significantly reduced. In addition, costunolide dose-dependently inhibited the generation of IL-6, TNF-α, IL-1β, and keratinocyte-derived cytokine (KC), as well as the expression of iNOS, in HKSA-induced macrophages. Furthermore, costunolide attenuated the phosphorylation of p38 MAPK and cAMP response element-binding protein (CREB). Collectively, our findings suggested that costunolide is a promising agent for alleviating bacterial-induced ALI via the inhibition of the MAPK signaling pathways.

Keywords: Costunolide; *Staphylococcus aureus*; pneumonia; macrophage; MAPK signaling

Acta Pharmacologica Sinica (2019) 40:1040–1048; https://doi.org/10.1038/s41401-018-0192-6

INTRODUCTION

Staphylococcus aureus (*S. aureus*) is one of the most clinically relevant bacterial pathogens and affects more than one-fifth of the world's population [1, 2]. *S. aureus* infection has been linked to a variety of pathologies, including sinusitis, osteomyelitis, and pneumonia, among others [3]. Furthermore, *S. aureus* is responsible for up to 10% of all cases of community-acquired pneumonia, with 20–40% of those attributable to hospital- or ventilator-associated infections [4, 5]. Notably, the emergence of new antibiotic-resistant strains, such as methicillin-resistant *S. aureus* (MRSA), has led to a resurgence of pneumonia incidence and mortality worldwide [6, 7]. Sepsis is a life-threatening condition induced by a severe host inflammatory response [8]. Sepsis in patients with *S. aureus* pneumonia is a primary contributor to shock, persistent high fever and even respiratory failure due to the cytokine storm. Because the occurrence of sepsis, especially in its more severe forms, is generally associated with a poorer outcome, mitigation of the pro-inflammatory response has been considered an important component of the treatment of *S. aureus* pneumonia and other infectious diseases [9, 10].

Decades of rigorous research have significantly advanced understanding of mechanisms that underlie the inflammatory response to *S. aureus* infection. It is well-established that the Toll-like receptors (TLRs), a family of transmembrane proteins that recognize and interact with pathogen-associated molecular patterns (PAMPs), play crucial roles in mobilizing the innate immune system against invading bacterial pathogens [11]. Recently, numerous studies have linked TLR2 to the *S. aureus*-induced inflammatory response, especially the production of pro-inflammatory cytokines. TLR2 is capable of identifying a wide range of structurally diverse pathogen-derived macromolecular structures, a feature that can be at least partially attributed to its ability to form heterodimers with various coreceptors [12]. In this regard, the heterodimerization of TLR2 with TLR1 or TLR6 has been shown to constitute a key step in the detection of *S. aureus* PAMPs by monocytes and macrophages [13, 14]. The recognition of PAMPs by TLR2 can trigger the recruitment of adapter molecules such as MyD88, which subsequently forms complexes with members of the interleukin-1 receptor-associated kinase (IRAK) family [14]. This complex formation leads to the generation of phosphorylated IRAK1 and its subsequent association with tumor necrosis factor receptor-associated factor (TRAF) 6, an E3 ubiquitin ligase [15]. TRAF6-dependent polyubiquitination drives the activation of transforming growth factor β-activated kinase (TAK) 1, a process that is also mediated by a group of regulatory subunits known as TAK1-binding proteins (TABs) [16, 17]. Eventually, activated TAK1 can upregulate the nuclear factor kappa light chain enhancer of activated B cells (NF-κB) and mitogen-activated protein kinase (MAPK) pathways, resulting in the production of nitric oxide (NO) and various pro-inflammatory cytokines, such as, among others, TNF-α, IL-1β, IL-6, and keratinocyte-derived cytokine (KC), which ultimately contribute to severe septic lung tissue damage in pneumonia patients [18]. These findings have formed the theoretical basis for the development of novel therapeutics against *S. aureus*-induced pneumonia and other infectious diseases.

[1]Department of Respiratory Medicine, Shanghai Ninth People's Hospital, Shanghai Jiao Tong University School of Medicine, Shanghai 200011, China; [2]Department of Infectious Diseases, The Fifth People's Hospital of Shanghai, Fudan University, Shanghai 200240, China and [3]Engineering Research Center of Cell & Therapeutic Antibody, Ministry of Education, School of Pharmacy, Shanghai Jiao Tong University, Shanghai 200240, China
Correspondence: Jian Wang (wangjian0628@163.com) or Feng Qian (fengqian@sjtu.edu.cn)
These authors contributed equally: Yun-tian Chen, Yao Du.

Received: 30 June 2018 Accepted: 1 November 2018
Published online: 15 January 2019

Costunolide is a sesquiterpene lactone that occurs naturally in plants such as *Saussureacostus* and *Lactuca sativa*. It has been used as an important herbal medicine ingredient in China, Japan, and India for breast cancer [19] and has also shown medicinal benefits for other types of malignancies, including hepatoma, intestinal carcinoma, and ovarian cancer [20–22]. Furthermore, costunolide exhibits significant fungicidal and anti-inflammatory properties [23]. These biochemical features make costunolide an attractive candidate for the treatment of bacterial infectious diseases. However, to the best of our knowledge, there have been no reports in the literature investigating the therapeutic effects of costunolide on *S. aureus* infection and pneumonia. Herein we report the evaluation of costunolide in a murine pneumonia model generated using heat-killed *S. aureus* (HKSA). Our experimental data indicated that costunolide could inhibit HKSA-induced neutrophil infiltration, cytokine secretion, and NO production, leading to significant attenuation of lung tissue injury. Costunolide also attenuated the activation of p38 MAPK and cAMP response element-binding protein (CREB). The results of the present study thus provide preliminary evidence supporting the therapeutic potential of costunolide for the treatment of *S. aureus*-associated pneumonia and other infectious diseases.

MATERIALS AND METHODS

Cell culture and preparation

Mouse bone marrow-derived macrophages (BMDMs) were prepared from C57BL/6 mice and cultured in DMEM (Sigma, St. Louis, MO, USA) with 10% FBS and 1% streptomycin-penicillin. All cell cultures were maintained at 37 °C with 5% CO_2. To prepare alveolar macrophages (AMs), bronchoalveolar lavage was collected and incubated at 37 °C with 5% CO_2 for 1 h to remove suspended cells. Then, the attached AMs were collected and pelleted. Fifty thousand AMs were plated in a 96-well-plate, or one million BMDMs were added to a 6-well-plate, which were then challenged with HKSA at 1×10^8 particles/mL.

Preparation of bacterial cells

S. aureus strain was grown overnight in Luria-Bertani (LB) medium at 37 °C with shaking (200 rpm). The culture was then diluted 100-fold in LB and grown to mid-log phase (O.D. 600 nm). Bacterial cells were pelleted at 1000 rpm with 30 min at 4 °C and washed twice with PBS. The bacterial concentration was measured by serially diluting the culture in PBS-Tween 20 (0.05%) followed by plating on LB-agar. After bacterial colonies were measured, heat-killed *S. aureus* (HKSA) was prepared by boiling the culture for 60 min and then stored at −80 °C.

In vivo model of acute lung injury

Male C57BL/6J mice of approximately 8–10 week of age were purchased from SLAC Laboratory Animal Corporation (Shanghai, China) and maintained at the Laboratory Animal Center of Shanghai Jiao Tong University (Shanghai, China) under 12-h light, 12-h dark cycles with free access to food and water. Costunolide was dissolved in vehicle consisting of 10% DMSO, 60% cremophor, 20% ethanol and 10% PBS. To assess the effect of costunolide on HKSA-induced lung injury, the mice were randomly separated into three groups: (1) injected with saline solution (Sham group); (2) injected with HKSA plus saline vehicle (HKSA+Vehicle); (3) injected with HKSA plus costunolide (HKSA+Cos). After being anesthetized, mice were intratracheally (i.t.) injected with HKSA (2×10^8 per each mouse) in 50 μL PBS. Costunolide (30 mg/kg) was intraperitoneally (i.p.) injected into the mice before HKSA challenge. After 8 h, the mice were sacrificed. BAL fluid (BALF) and lung tissues were collected for the following assays. To determine whether costunolide has therapeutic effects, we treated mice with costunolide after HKSA challenge. First, mice were i.t. injected with HKSA (2×10^8 per each mouse) to induce pulmonary inflammation. After 1 h, the mice were i.p. injected with 30 mg/kg of costunolide, and acute lung injury was evaluated at 24 h.

Bronchoalveolar lavage (BAL)

All mice were sacrificed eight or twenty-four hours after HKSA challenge, followed by harvesting of tracheae and lungs. A small-caliber tube was then inserted into the airway of each trachea and fixed. Next, the trachea was filled with 1 mL of PBS containing 0.1% bovine serum albumin and aspirated gently. BAL fluid was collected from each euthanized animal by lavage twice as described above and pooling the resultant liquid. The BAL fluid samples were then centrifuged at 4 °C and $1000 \times g$ for 5 min. The supernatants were collected and stored at −80 °C for further experiments [24].

Lung wet/dry weight ratio

The harvested murine lungs were weighed, dried at 60 °C for 3 days, and then weighed again. The weight ratio of the wet to dry lung was calculated.

Myeloperoxidase (MPO)

Thiobarbituric acid (TBA) was added to the lung tissue homogenates. The mixture was centrifuged and the supernatant measured spectrophotometrically to evaluate myeloperoxidase activity. MPO activity was calculated as the absorbance change per gram of lung tissue [25].

Pulmonary histopathology

The lung tissues were fixed in normal 4% buffered formalin for 48 h, dehydrated in graded alcohol, embedded in paraffin wax, stained with hematoxylin and eosin (H&E), and then visualized under a light microscope for histopathological assessment [26].

Flow cytometry

The lungs were lavaged, and total cells in BAL were calculated. The BAL was centrifuged ($300 \times g$, 5 min), and the supernatants were stored at −80 °C for further analysis. Pulmonary infiltrated cells were stained with anti-Ly6G-FITC, anti-CD11c-APC, and anti-F4/80-PE-Cy7 (eBiosciences, San Diego, CA, USA), and macrophage isolation was performed using a FACS Aria III cell sorter (BD Biosciences, San Jose, NJ, USA). Neutrophils (Ly6G+) and macrophages (CD11c+F4/80+) were identified. Data were analyzed with FlowJo (Tree Star, Ashland OR, USA) software.

NO metabolite determination

Briefly, 50 μL of each BAL supernatant was mixed with a 50-μL volume of 1% *w/v* sulfanilamide and 5% *w/v* phosphoric acid solution. The resultant mixture was incubated for 10 min in the dark, followed by the addition of 50 μL of 0.1% *w/v* N-(naphthyl) ethyl-enediamidedihydrochloride. The sample was incubated at room temperature in the dark for another 10 min. The absorbance at 550 nm was measured to calculate the level of NO using a $NaNO_2$ standard curve.

Enzyme-linked immunosorbent assay (ELISA)

ELISA was used to detect the concentrations of different cytokines and chemokines. The concentrations of tumor necrosis factor alpha (TNF-α), interleukin-1 beta (IL-1β), interleukin-6 (IL-6), and KC were measured and analyzed using Quantikine ELISA kits (R&D SYSTEMS, Minneapolis, MN, USA).

Western blot analysis

Equal amounts of proteins from cell lysates were denatured, electrophoresed on 10% or 12% SDS-polyacrylamide gels under a constant voltage of 100 V (Bio-Rad, Hercules, CA, USA), and then transferred to nitrocellulose membranes (Millipore, Billerica, MA,

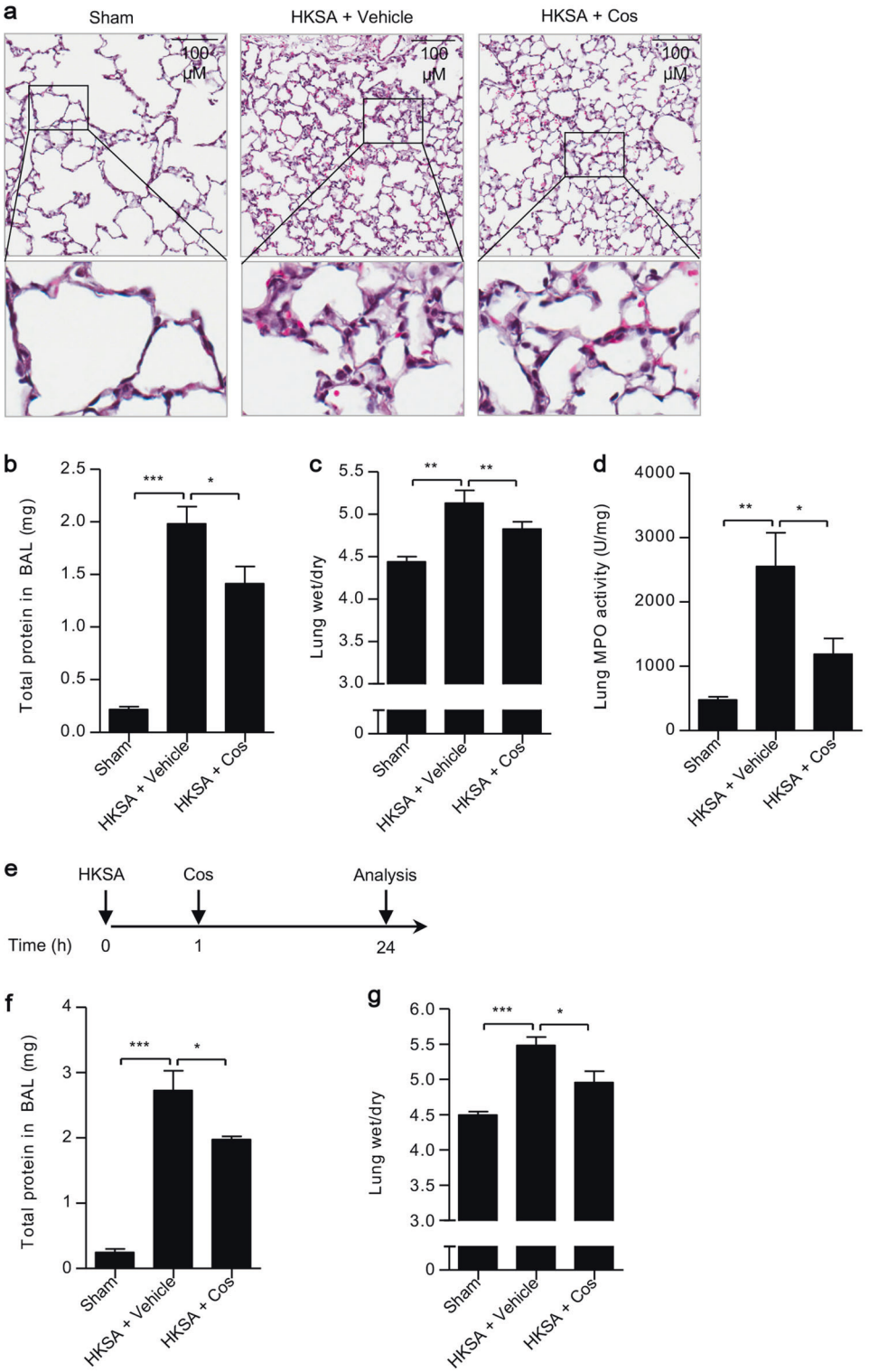

Fig. 1 Costunolide ameliorates HKSA-induced acute lung injury. Mice (C57BL/6, $n = 5$/group) were intratracheally (i.t.) injected with HKSA (2×10^8 per each mouse) in 50 μl PBS. Costunolide (30 mg/kg) was intraperitoneally (i.p.) injected into mice before HKSA challenge. After 8 h, the mice were sacrificed and the lungs lavaged. Lung tissue slides were stained with H&E and analyzed under microscopy at a magnification of 200 × (**a**). (**b**) The total protein in bronchoalveolar lavage (BAL) was measured to evaluate lung permeability. (**c**) The lung wet to dry ratio was detected. (**d**) The lung tissues were homogenized and the MPO assay performed to identify neutrophil infiltration. (**e**) Schematic timeline showing the therapeutic effect of costunolide on acute lung injury. Mice (C57BL/6, $n = 5$/group) were first i.t. injected with 2×10^8 of HKSA. After 1 h, the mice were treated with 30 mg/kg of costunolide by i.p. injection. (**f**) The total protein in BAL was measured to evaluate lung permeability. (**g**) The lung wet to dry ratio was analyzed after 24 h. Data are the mean ± SEM. $^*P < 0.05$, $^{**}P < 0.01$, $^{***}P < 0.001$

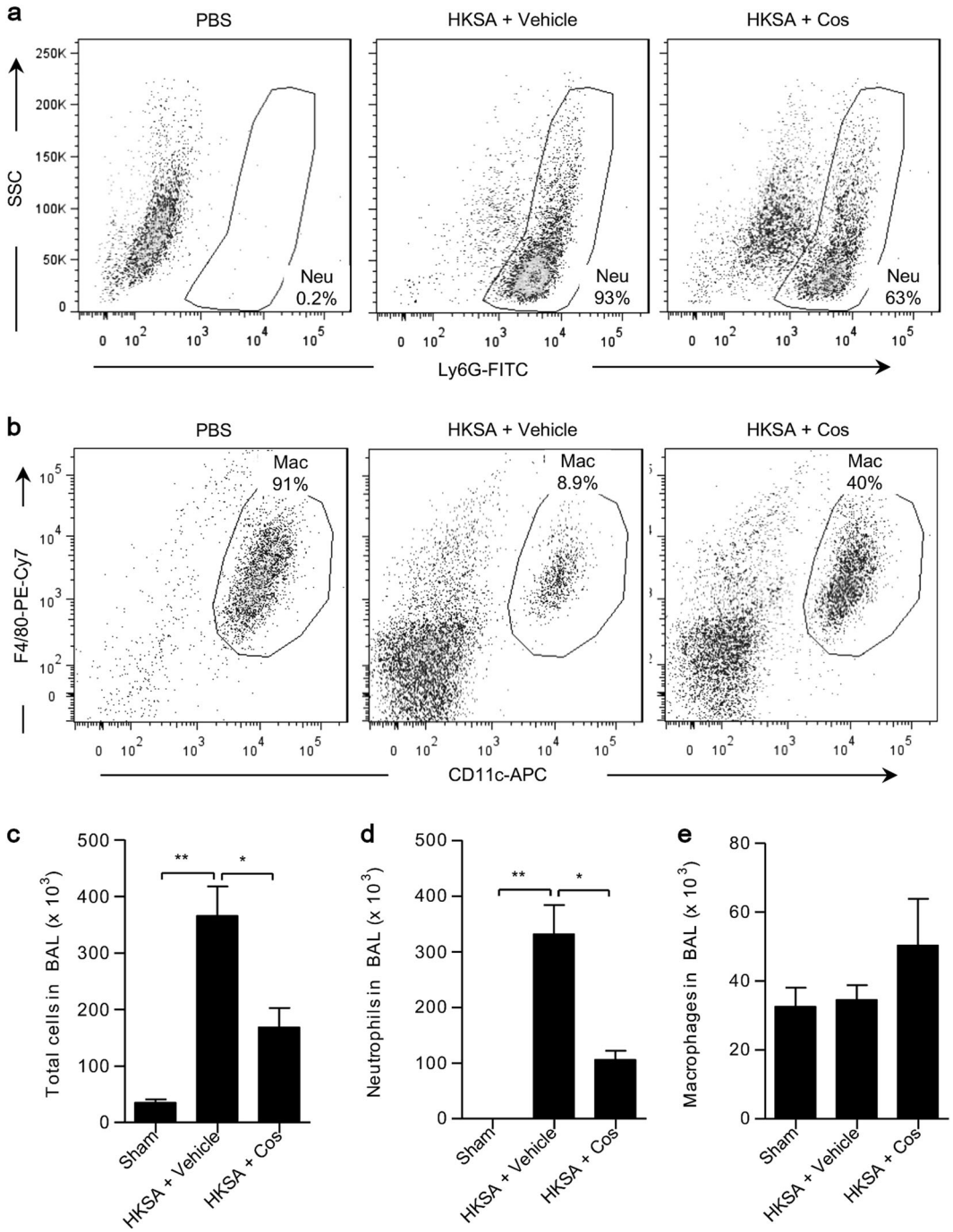

Fig. 2 Costunolide attenuates HKSA-induced pulmonary neutrophil infiltration. Mice ($n = 5$/group) were intratracheally (i.t.) treated with HKSA (2×10^8 per each mouse), which were pretreated with 30 mg/kg of costunolide. After 8 h, the lungs were lavaged and total cells in BAL were calculated. Pulmonary infiltrated cells were stained with anti-Ly6G-FITC, anti-CD11c-APC, and anti-F4/80-PE-Cy7, and detected by flow cytometry. (**a**) Neutrophils ($Ly6G^+$) and (**b**) macrophages ($CD11c^+F4/80^+$) were identified. Total cells in BAL were counted (**c**). The numbers of neutrophils (**d**) and macrophages (**e**) were calculated based on the percentage of the cells. Data are the mean ± SEM. $^*P < 0.05$, $^{**}P < 0.01$

USA). After blocking at room temperature for 2 h, proteins on the membrane were incubated with antibodies against iNOS, β-Actin, Phospho-NF-κB p65 (Ser536), NF-κB p65, Phospho-Akt (Thr308), IκB, Akt (pan), Phospho-p38 MAPK (Thr180/Tyr182), p38 MAPK, Phospho-p44/42 MAPK (Erk1/2) (Thr202/Tyr204), p44/42 MAPK (Erk1/2), Phospho-SAPK/JNK (Thr183/Tyr185), SAPK/JNK, Phospho-CREB (Ser133), and CREB (Cell Signaling, Danvers, MA, USA). After washing, the membranes were further incubated with horseradish peroxide-conjugated secondary antibodies for 2 h, and bands of different proteins were visualized using the Odyssey Infrared Imaging System (Odyssey CLx, Medford, MA, USA).

Statistical analysis

Results are expressed as the means ± SEM of at least three independent experiments. The Student's *t*-test was used for comparisons between two groups, whereas one-way ANOVA followed by the post hoc Tukey test was employed for comparison of three or more groups. $P < 0.05$ was considered statistically significant.

RESULTS

Costunolide ameliorates HKSA-induced acute lung injury

To determine the role of costunolide in acute lung injury, mice were intratracheally injected with HKSA to induce septic lung tissue injury, which initiates a septic inflammatory cascade. Histological examinations confirmed that the mice in the vehicle group showed significant pathologic changes in the lungs, including destruction of the normal tissue architecture, alveolar wall thickening, and inflammatory cell infiltration (Fig. 1a). In contrast, the mice in the treatment group exhibited significantly less lung injury (Fig. 1a). The total protein in bronchoalveolar lavage fluid was measured to evaluate lung permeability. The protein concentration in the BALF was notably increased in mice treated with HKSA, and this increase was reduced by costunolide treatment (Fig. 1b).

Next, we investigated whether the mice showed any signs of edema formation in their lungs by determining the lung wet/dry ratio. The vehicle group showed a significant increase in lung wet/dry ratios following inoculation of HKSA compared with the sham group. However, administration of costunolide was able to effectively decrease the lung wet/dry ratio (Fig. 1c) in HKSA-infected mice.

MPO activity in lung tissues can be considered a marker of neutrophil infiltration. HKSA treatment increased the MPO activity in lung tissues; however, this effect was significantly attenuated by costunolide treatment (Fig. 1d).

To determine whether costunolide has therapeutic effects on HKSA-induced acute lung injury, we first i.t. injected mice with HKSA. After 1 h, the mice were treated with costunolide by i.p. injection (Fig. 1e). Lung injury was evaluated at 24 h after HKSA treatment. Costunolide treatment significantly decreased the pulmonary total protein (Fig. 1f) and the lung wet/dry ratio (Fig. 1g).

Costunolide attenuates HKSA-induced pulmonary neutrophil infiltration

Total cells, neutrophils and macrophages in BALF were counted by staining with anti-Ly6G-FITC (Fig. 2a), as well as anti-CD11c-APC and anti-F4/80-PE-Cy7 (Fig. 2b). Compared with the Sham group, total cells (Fig. 2c) and neutrophils (Fig. 2d) were increased in mice treated with HKSA alone. Additionally, pretreatment with costunolide induced a marked decrease in the total cells (Fig. 2c) and neutrophils (Fig. 2d) in BALF. However, costunolide showed no detectable effect on the number of AMs (Fig. 2c).

Costunolide reduces HKSA-induced cytokine and chemokine production

The mice were pretreated with costunolide before HKSA challenge. After 8 h of HKSA treatment, the lung lobes were lavaged and cytokines and chemokine detected by ELISA. HKSA challenge significantly increased the levels of IL-6 (Fig. 3a), TNF-α (Fig. 3b), IL-1β (Fig. 3c), and KC (Fig. 3d) in BALF, whereas pretreatment with costunolide had a mitigating effect on the production of these cytokines and chemokines.

Costunolide inhibits the production of cytokines and chemokines in BMDMs and AMs

The production of IL-6 (Fig. 4a and e), TNF-α (Fig. 4b and f), IL-1β (Fig. 4c and g), and KC (Fig. 4d and h) in the culture supernatants of BMDMs and AMs was measured by ELISA. HKSA stimulation significantly initiated the expression of cytokines and chemokines. However, costunolide considerably inhibited HKSA-induced cytokine and chemokine production in a dose-dependent manner.

Costunolide reduces iNOS expression and nitric oxide (NO) generation

BMDMs were pretreated with different concentrations of costunolide (0, 3, 10, and 30 μM) for 30 min and then coincubated with HKSA for 18 h. Western blotting demonstrated that the expression of iNOS was dramatically upregulated in the vehicle group following HKSA infection. However, this effect was significantly alleviated by costunolide in a dose-dependent manner (Fig. 5a, b). The level of NO in the BAL fluid showed a similar trend (Fig. 5c).

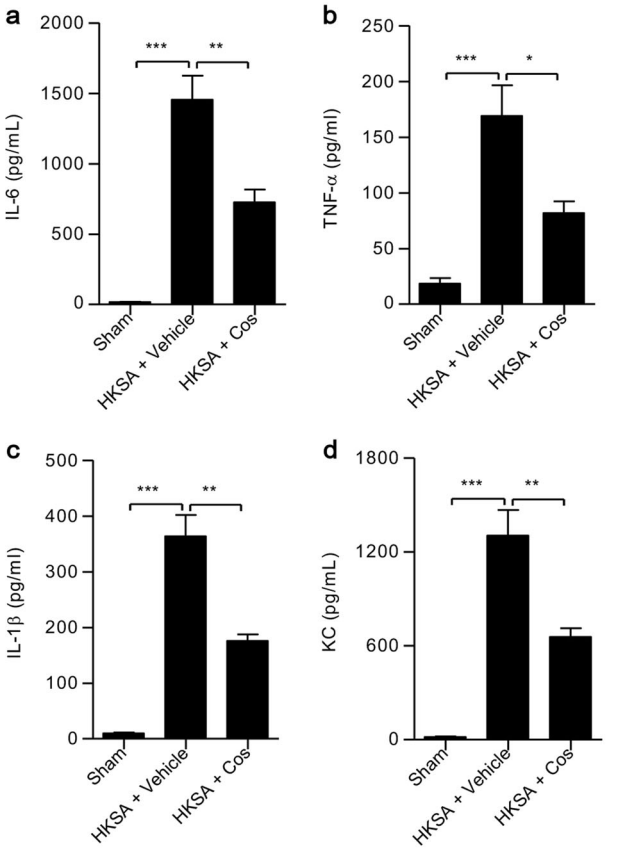

Fig. 3 Costunolide reduces HKSA-induced cytokine and chemokine production. Mice ($n = 5$/group) were intraperitoneally injected with costunolide (30 mg/kg) and intratracheally (i.t.) challenged with HKSA (2×10^8 per each mouse). After 8 h, the lungs were lavaged and cytokines and chemokine detected by ELISA. IL-6 (**a**), TNF-α (**b**), IL-1β (**c**), and KC (**d**) were measured. Data are the mean ± SEM. $^*P < 0.05$, $^{**}P < 0.01$, $^{***}P < 0.001$

Costunolide inhibits the phosphorylation of p38 MAPK and CREB in response to HKSA stimulation

TLR2 is a membrane-anchor TLR that is involved in the host recognition of *S. aureus*, which leads to activation of the NF-kB and MAPK signaling pathways. Therefore, we assessed whether costunolide has an effect on these signaling pathways. The expression of Phos-p65, Total-p65, IkB (Fig. 6a), Phos-Akt, Total-Akt (Fig. 6b), Phos-p38, Total-p38, Phos-ERK, Total-ERK, Phos-JNK, Total-JNK, Phos-CREB, and Total-CREB (Fig. 6c) were detected by western blot analysis, respectively. The results showed that the administration of costunolide significantly attenuated HKSA-triggered phosphorylation of p38 and CREB in a concentration-dependent manner (Fig. 6d and e). However, there were no appreciable effects on the phosphorylation of other kinases.

DISCUSSION

In this study, we investigated the protective effects of costunolide on *S. aureus*-induced septic pulmonary injury in a mouse model generated by the intratracheal administration of HKSA. Research has indicated that the detection and subsequent immune

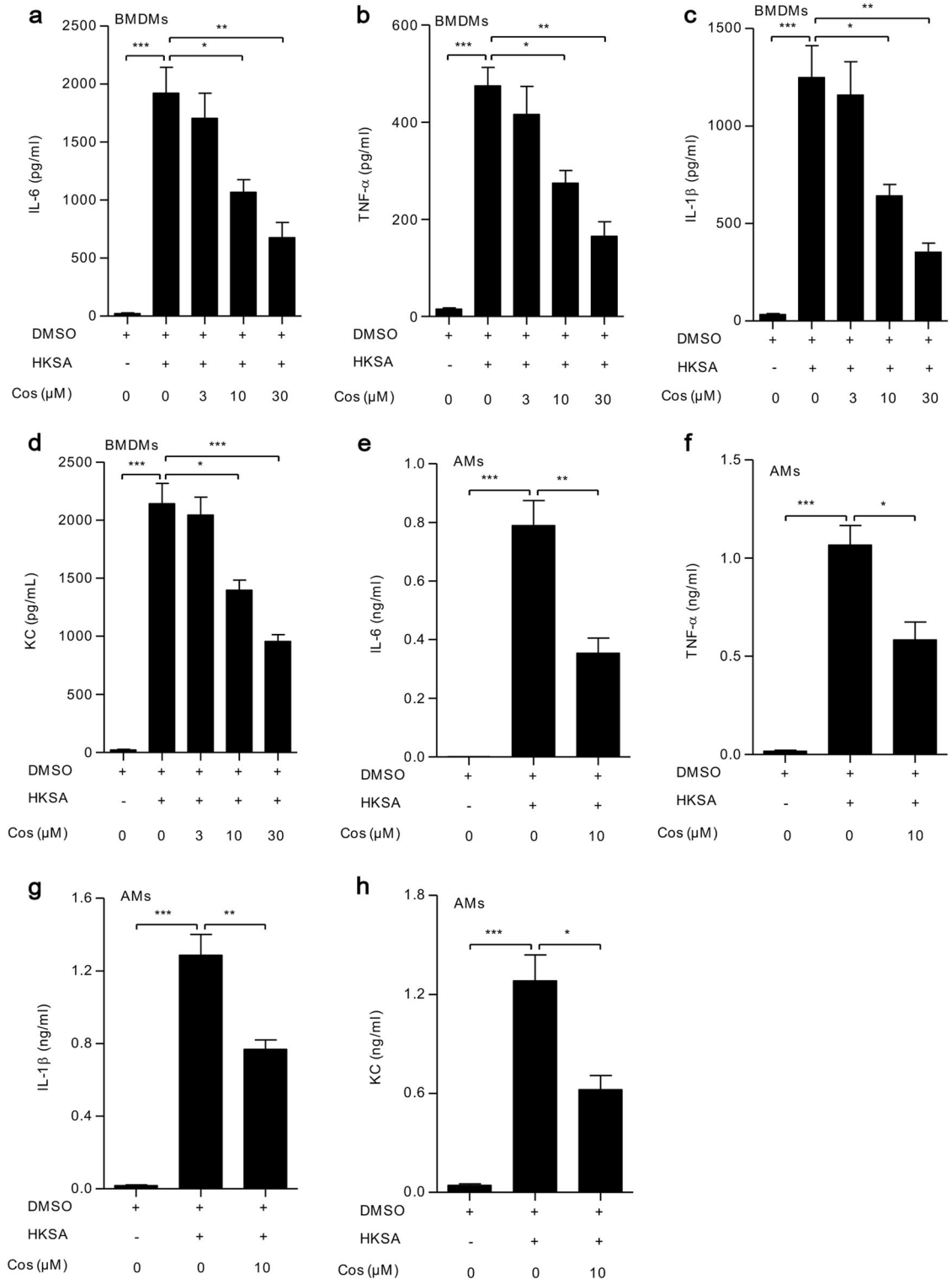

Fig. 4 Costunolide inhibits the production of cytokines and chemokines in BMDMs and AMs. BMDMs (1×10^6) from C57BL/6 mice were pretreated with costunolide at 0, 3, 10, and 30 μM for 30 min (**a**–**d**), or AMs (0.5×10^6) were pretreated with 10 μM of costunolide for 30 min (**e**–**h**) then stimulated with HKSA (1×10^8 particles/ml) for 18 h. The production of IL-6 (**a** and **e**), TNF-α (**b** and **f**), IL-1β (**c** and **g**), and KC (**d** and **h**) was measured by ELISA. The experiments were independently repeated at least three times. Data are the mean ± SEM. $^*P < 0.05$, $^{**}P < 0.01$, $^{***}P < 0.001$

response to staphylococcal components, particularly cell wall constituents and secreted proteins, play a central role in initiating the inflammation cascade responsible for the destruction of lung tissues [27]. Our experiment data indicated that the administration of costunolide greatly alleviated lung injury caused by *S. aureus* infection in mice. Further studies revealed that costunolide could significantly suppress the infiltration of pulmonary neutrophils, production of cytokines and chemokines, and the generation of

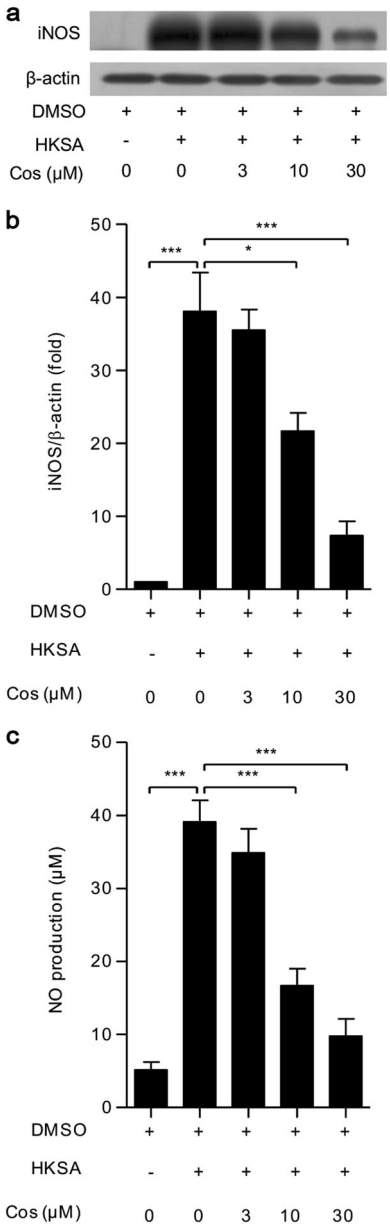

Fig. 5 Costunolide reduces iNOS expression and nitro oxide (NO) generation. BMDMs (1×10^6) were pretreated with costunolide at 0, 3, 10, and 30 μM for 30 min and then challenged with HKSA (1×10^8 particles/ml) for 18 h. (**a**) Western blotting was conducted to detect the expression of iNOS using anti-iNOS and β-actin antibodies. (**b**) Quantitative assay of iNOS detected using ImageJ software. (**c**) The production of NO in the supernatant was measured using the NO assay kit (Griess reagents). The experiments were independently performed at least three times. Data are the mean ± SEM. *$P < 0.05$, **$P < 0.01$, ***$P < 0.001$

NO, all of which contributed to a reduced inflammatory response. Mechanistically, we presented evidence linking the anti-inflammatory properties of costunolide to its ability to suppress the MAPK pathway by inhibiting the phosphorylation of p38 and CREB. Taken together, our results provide convincing evidence that costunolide can serve as an effective therapeutic agent against *S. aureus*-induced pulmonary inflammation.

Our findings demonstrate that costunolide exerts a strong inhibitory effect on HKSA-induced septic lung injury via the MAPK pathway, echoing the results of many other studies. For example, Rayan et al. reported that costunolide could suppress the activity of nitric NO synthase and the production of IL-1 and IL-6 in activated murine microglia by downregulating the MAPK pathway, which could provide cerebroprotection in neuroinflammatory diseases [28]. In contrast, costunolide has also been shown to attenuate the NF-κB pathway. Buttutini and coworkers demonstrated that the administration of costunolide in mice with pulmonary pleurisy significantly reduced the secretion of pro-inflammatory cytokines and mitigated tissue damage as a result of decreased NF-κB activity [29]. It is worth mentioning that costunolide-dependent inhibition of the MAPK and NF-κB pathways could also contribute to the anti-tumor properties of the compound. It has been suggested that suppression of the NF-κB pathway by costunolide can diminish the expression of metalloproteinase (MMP)-9 and concomitantly reduce the invasive capacity of MCF-7 breast cancer cells [30]. However, in the study by Lee et al., the inhibitory effect of costunolide on receptor activator of nuclear factor kappa-B ligand (RANKL)-stimulated osteoclastic differentiation of bone marrow cells did not seem to involve the modulation of either the MAPK or the NF-κB pathway, but rather occurred via the transcriptional deactivation of c-Fos [31]. Taken together, these findings point to the regulatory versatility of costunolide and suggest that it might be able to interact with different targets to elicit a range of biological effects in different cellular contexts.

There is mounting evidence that both the MAPK and NF-κB pathways play central roles in the propagation of inflammation and resultant aggravation of tissue injuries [32]. As a result, the two signaling pathways have been rigorously investigated as potential therapeutic targets. Given the reduced activation of MAPK signaling pathway, costunolide may target upstream molecules of these signaling pathways. Pan and colleagues have reported that xyloketal B, a polycyclic aromatic compound derived from Xylaria sp. fungus, can effectively reduce the levels of reactive oxygen species (ROS) and pro-inflammatory cytokines by blocking the ROS/TLR4/NF-κB signaling cascade, thus offering effective neuroprotection in a mouse model of hypoxic-ischemic brain injury [33]. Treatment of human neuroblastoma cells with cyanadin, a plant-derived polyaromatic and polyphenolic pigment, greatly stimulates the production of cytoprotective enzymes and simultaneously decreases NF-κB activity by downregulating the upstream TLR4/NOX pathway [34]. Both NF-κB and MAPK signaling have also been shown to be targeted by carnosic acid, ameliorating inflammatory response and joint damage in arthritic rats [35]. Given the ability of costunolide to inhibit MAPK and CREB, we envision that it could be used in conjunction with other anti-inflammatory agents that function via a different molecular mechanism to provide enhanced therapeutic benefits. Indeed, a recent study conducted by Martinez-micaelo demonstrated that simultaneous inhibition of cyclo-oxygenase and the NF-κB pathway synergistically alleviated the LPS-induced inflammatory response in human macrophages [36]. As a result, costunolide-based combination drug therapies that simultaneously target several parallel signaling pathways could constitute a promising strategy against inflammatory diseases.

The generation of NO and pro-inflammatory cytokines is thought to play a direct role in tissue damage in the pathogenesis of S. *aureus* pneumonia. For instance, it has been reported that TNF-α can act on receptor interacting protein 3 to promote necroptosis of alveolar cells infected by *S. aureus* [37]. The use of an antibody that specifically targets TNF-α, or, in a similar manner, another implicated pro-inflammatory cytokine, clearly could also be a putative strategy for managing inflammatory complications in *S. aureus*-induced pneumonia. However, a major disadvantage that limits the clinical potential of such anti-inflammatory antibodies is their relatively high production costs. In comparison, costunolide is easily available from plant sources and exhibits a favorable safety profile, making it a viable candidate in such

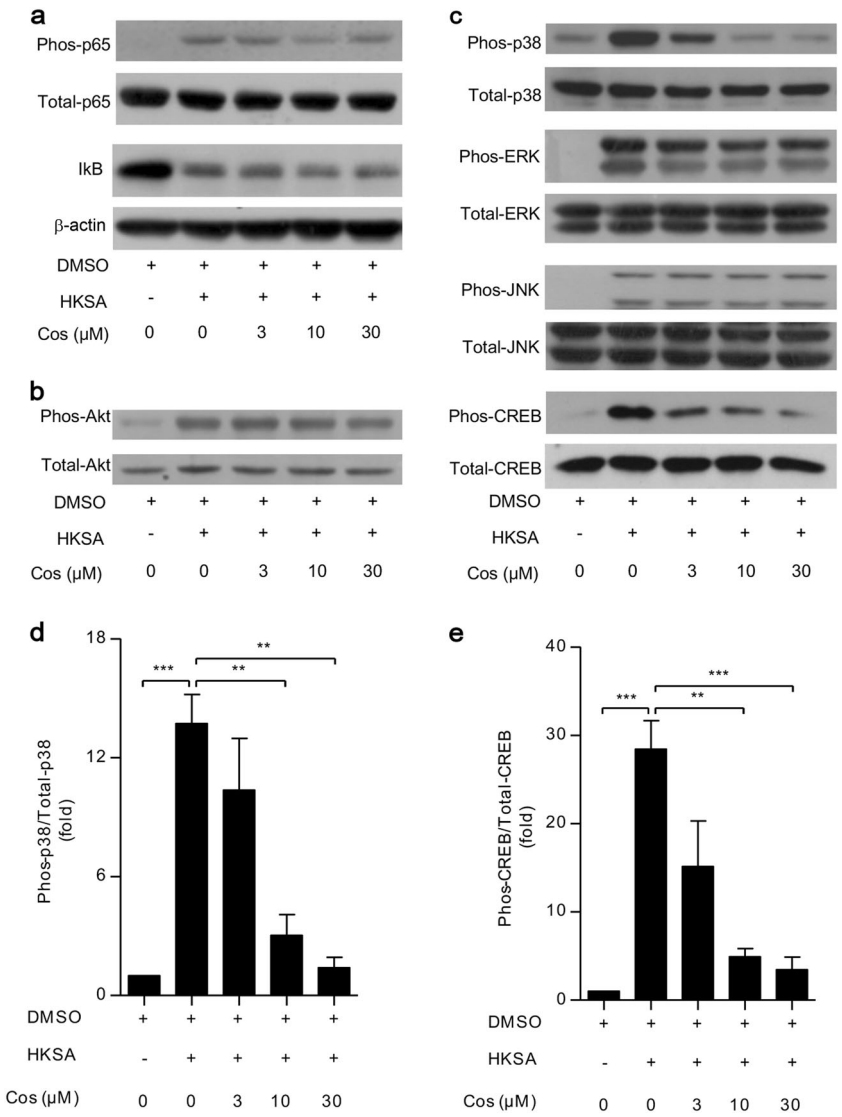

Fig. 6 Costunolide inhibits the phosphorylation of p38 MAPK and CREB in response to HKSA stimulation. BMDMs (1×10^6) were incubated with costunolide at 0, 3, 10, and 30 μM for 30 min and then challenged with HKSA (1×10^8 particles/ml) for an additional 30 min. Cell signaling was screened by Western blotting. (**a**) The phosphorylation of p65, total p65, IκB, and β-actin was detected. (**b**) The phosphorylation of Akt (Ser308) and total Akt was identified. (**c**) The phosphorylation of p38 MAPK (p38), ERK, JNK, and CREB and their total proteins were measured. The quantitative assay for phosphorylation of p38 MAPK (**d**) and CREB (**e**) was carried out using ImageJ software. The experiments were independently repeated at least three times. Data are the mean ± SEM. $^{**}P < 0.01$, $^{***}P < 0.001$

applications. Therefore, our findings may provide a new agent for the cure of bacterial-mediated pneumonia or other inflammatory diseases.

ACKNOWLEDGEMENTS

This work was supported by the National Key Research and Development Program of China (2017YFC0908500) and National Natural Science Foundation of China (81773741, 81573438, 31741038, and 31770921).

AUTHOR CONTRIBUTIONS

FQ, JW, YC, and YD designed the study and drafted the manuscript. YC, YD, BZ, LG, and KY performed the experiments and data analysis. LS provided suggestions regarding the experimental design, data analysis and discussion.

ADDITIONAL INFORMATION

Competing interests: The authors declare no competing interests.

REFERENCES

1. Kluytmans J, van Belkum A, Verbrugh H. Nasal carriage of Staphylococcus aureus: epidemiology, underlying mechanisms, and associated risks. Clin Microbiol Rev. 1997;10:505–20.
2. Dzidic S, Bedekovic V. Horizontal gene transfer-emerging multidrug resistance in hospital bacteria. Acta Pharmacol Sin. 2003;24:519–26.
3. Lowy FD. Staphylococcus aureus infections. N Engl J Med. 1998;339:520–32.
4. Fang GD, Fine M, Orloff J, Arisumi D, Yu VL, Kapoor W, et al. New and emerging etiologies for community-acquired pneumonia with implications for therapy. A prospective multicenter study of 359 cases. Med (Baltim). 1990;69:307–16.
5. Sibila O, Rodrigo-Troyano A, Shindo Y, Aliberti S, Restrepo MI. Multidrug-resistant pathogens in patients with pneumonia coming from the community. Curr Opin Pulm Med. 2016;22:219–26.
6. Khan A, Wilson B, Gould IM. Current and future treatment options for community-associated MRSA infection. Expert Opin Pharmacother. 2018;19:457–70.
7. Wunderink RG, Waterer G. Advances in the causes and management of community acquired pneumonia in adults. BMJ. 2017;358:j2471.
8. Wang K, Lai C, Li T, Wang C, Wang W, Ni B, et al. Basic fibroblast growth factor protects against influenza A virus-induced acute lung injury by recruiting neutrophils. J Mol Cell Biol. 2017. [Epub ahead of print].

9. Gudiol C, Cuervo G, Shaw E, Pujol M, Carratala J. Pharmacotherapeutic options for treating Staphylococcus aureus bacteremia. Expert Opin Pharmacother. 2017;18:1947–63.
10. Jiang KF, Zhao G, Deng GZ, Wu HC, Yin NN, Chen XY, et al. Polydatin ameliorates Staphylococcus aureus-induced mastitis in mice via inhibiting TLR2-mediated activation of the p38 MAPK/NF-kappaB pathway. Acta Pharmacol Sin. 2017;38:211–22.
11. Trinchieri G, Sher A. Cooperation of Toll-like receptor signals in innate immune defence. Nat Rev Immunol. 2007;7:179–90.
12. Farhat K, Riekenberg S, Heine H, Debarry J, Lang R, Mages J, et al. Heterodimerization of TLR2 with TLR1 or TLR6 expands the ligand spectrum but does not lead to differential signaling. J Leukoc Biol. 2008;83:692–701.
13. Kubica M, Guzik K, Koziel J, Zarebski M, Richter W, Gajkowska B, et al. A potential new pathway for Staphylococcus aureus dissemination: the silent survival of S. aureus phagocytosed by human monocyte-derived macrophages. PLoS ONE. 2008;3:e1409.
14. Lin SC, Lo YC, Wu H. Helical assembly in the MyD88-IRAK4-IRAK2 complex in TLR/IL-1R signalling. Nature. 2010;465:885–90.
15. Walsh MC, Lee J, Choi Y. Tumor necrosis factor receptor- associated factor 6 (TRAF6) regulation of development, function, and homeostasis of the immune system. Immunol Rev. 2015;266:72–92.
16. Vijay K. Toll-like receptors in immunity and inflammatory diseases: past, present, and future. Int Immunopharmacol. 2018;59:391–412.
17. Abreu MT. Toll-like receptor signalling in the intestinal epithelium: how bacterial recognition shapes intestinal function. Nat Rev Immunol. 2010;10:131–44.
18. Qian F, Deng J, Gantner BN, Flavell RA, Dong C, Christman JW, et al. Map kinase phosphatase 5 protects against sepsis-induced acute lung injury. Am J Physiol Lung Cell Mol Physiol. 2012;302:L866–74.
19. Ateba SB, Ngeu ST, Mvondo MA, Tchoumtchoua J, Awounfack CF, Krenn L, et al. Natural terpenoids against female breast cancer: a 5-year recent research. Curr Med Chem. 2018;18:1947–63.
20. Mori H, Kawamori T, Tanaka T, Ohnishi M, Yamahara J. Chemopreventive effect of costunolide, a constituent of oriental medicine, on azoxymethane-induced intestinal carcinogenesis in rats. Cancer Lett. 1994;83:171–5.
21. Chen HC, Chou CK, Lee SD, Wang JC, Yeh SF. Active compounds from Saussurea lappa Clarks that suppress hepatitis B virus surface antigen gene expression in human hepatoma cells. Antivir Res. 1995;27:99–109.
22. Yang YI, Kim JH, Lee KT, Choi JH. Costunolide induces apoptosis in platinum-resistant human ovarian cancer cells by generating reactive oxygen species. Gynecol Oncol. 2011;123:588–96.
23. Duraipandiyan V, Al-Harbi NA, Ignacimuthu S, Muthukumar C. Antimicrobial activity of sesquiterpene lactones isolated from traditional medicinal plant, Costus speciosus (Koen ex.Retz.) Sm. BMC Complement Altern Med. 2012;12:13.
24. Wu YX, He HQ, Nie YJ, Ding YH, Sun L, Qian F. Protostemonine effectively attenuates lipopolysaccharide-induced acute lung injury in mice. Acta Pharmacol Sin. 2018;39:85–96.
25. He HQ, Wu YX, Nie YJ, Wang J, Ge M, Qian F. LYRM03, an ubenimex derivative, attenuates LPS-induced acute lung injury in mice by suppressing the TLR4 signaling pathway. Acta Pharmacol Sin. 2017;38:342–50.
26. Ding YH, Song YD, Wu YX, He HQ, Yu TH, Hu YD, et al. Isoalantolactone suppresses LPS-induced inflammation by inhibiting TRAF6 ubiquitination and alleviates acute lung injury. Acta Pharmacol Sin. 2018. [Epub ahead of print].
27. Qian F, Deng J, Wang G, Ye RD, Christman JW. Pivotal role of mitogen-activated protein kinase-activated protein kinase 2 in inflammatory pulmonary diseases. Curr Protein Pept Sci. 2016;17:332–42.
28. Rayan NA, Baby N, Pitchai D, Indraswari F, Ling EA, Lu J, et al. Costunolide inhibits proinflammatory cytokines and iNOS in activated murine BV2 microglia. Front Biosci (Elite Ed). 2011;3:1079–91.
29. Butturini E, Di Paola R, Suzuki H, Paterniti I, Ahmad A, Mariotto S, et al. Costunolide and Dehydrocostuslactone, two natural sesquiterpene lactones, ameliorate the inflammatory process associated to experimental pleurisy in mice. Eur J Pharmacol. 2014;730:107–15.
30. Kim HR, Kim JM, Kim MS, Hwang JK, Park YJ, Yang SH, et al. Saussurea lappa extract suppresses TPA-induced cell invasion via inhibition of NF-kappaB-dependent MMP-9 expression in MCF-7 breast cancer cells. BMC Complement Altern Med. 2014;14:170.
31. Cheon YH, Song MJ, Kim JY, Kwak SC, Park JH, Lee CH, et al. Costunolide inhibits osteoclast differentiation by suppressing c-Fos transcriptional activity. Phytother Res. 2014;28:586–92.
32. McGuire VA, Arthur JS. Subverting toll-like receptor signaling by bacterial pathogens. Front Immunol. 2015;6:607.
33. Pan N, Lu LY, Li M, Wang GH, Sun FY, Sun HS, et al. Xyloketal B alleviates cerebral infarction and neurologic deficits in a mouse stroke model by suppressing the ROS/TLR4/NF-kappaB inflammatory signaling pathway. Acta Pharmacol Sin. 2017;38:1236–47.
34. Thummayot S, Tocharus C, Jumnongprakhon P, Suksamrarn A, Tocharus J. Cyanidin attenuates Abeta25-35-induced neuroinflammation by suppressing NF-kappaB activity downstream of TLR4/NOX4 in human neuroblastoma cells. Acta Pharmacol Sin. 2018;39:1439–52.
35. Liu M, Zhou X, Zhou L, Liu Z, Yuan J, Cheng J, et al. Carnosic acid inhibits inflammation response and joint destruction on osteoclasts, fibroblast-like synoviocytes, and collagen-induced arthritis rats. J Cell Physiol. 2018;233:6291–303.
36. Martinez-Micaelo N, Gonzalez-Abuin N, Terra X, Richart C, Ardevol A, Pinent M, et al. Omega-3 docosahexaenoic acid and procyanidins inhibit cyclo-oxygenase activity and attenuate NF-kappaB activation through a p105/p50 regulatory mechanism in macrophage inflammation. Biochem J. 2012;441:653–63.
37. Wen SH, Lin LN, Wu HJ, Yu L, Lin L, Zhu LL, et al. TNF-alpha increases Staphylococcus aureus-induced death of human alveolar epithelial cell line A549 associated with RIP3-mediated necroptosis. Life Sci. 2018;195:81–6.